Polarimetric characterization of bismuth thin films deposited by laser ablation

Rafael Espinosa-Luna,[1,*] Enrique Camps,[2] Dagoberto Cardona,[2] and Elder De la Rosa[1]

[1]Centro de Investigaciones en Óptica, Apdo. Postal 1-948, León, Guanajuato 37150, Mexico

[2]Instituto Nacional de Investigaciones Nucleares, Departamento de Física, Apdo. Postal 18-1027, México D.F. 11801, Mexico

*Corresponding author: reluna@cio.mx

Received 23 August 2012; revised 12 November 2012; accepted 16 November 2012;
posted 16 November 2012 (Doc. ID 174766); published 13 December 2012

A Mueller–Stokes analysis is applied to pure bismuth thin film samples prepared by the laser ablation technique by using a polarimeter with a 632.8 nm continuum wavelength laser. The complex refractive index is determined in the range of 250–1100 nm. Results from the Mueller matrix show the high sensitivity of diattenuation and polarizance parameters as a function of the sample thickness and the incidence angle, except at the pseudo-Brewster angle, where they exhibit the same value. Results show that the knowledge of the polarimetric response, with appropriate incident polarization states, could be used to design photonic Bi-based devices for several applications. Polarization dependence is the result of changes on the surface morphology as a result of the small value of the skin depth.

OCIS codes: 310.5448, 310.6860, 160.4760.

1. Introduction

Bismuth (Bi) is a semimetal that has been studied extensively over the last 50 years, and its optical, electronic, and morphological properties have been determined [1–6]. Recently, it has attracted attention again due to its unique properties at a low-dimensional scale in medical applications [7,8], thermoelectric and switches devices [9,10], and diverse areas like electrodes, sensors, and detectors [11]. Thin films have been prepared by different methods, including low energy cluster beam deposition [12], thermal evaporation [13], and sputtering [14]. Less attention has been received by films prepared by laser ablation, also called pulsed laser deposition (PLD) [14–16]. The basic idea of the technique is to exploit high-power laser pulses in order to evaporate a small amount of matter from a solid target. The rapid superheating at the subsurface due to coupling and transfer of energy from the laser beam to the target materials leads to catastrophic vaporization and explosion, resulting in the generation of atomized droplets and highly ionized plasma. The plasma and the liquid droplets move at high speed and are quenched on a suitably positioned substrate. We believe the PLD technique could be used to get pure Bi thin film samples, which can be used for different photonic applications at room conditions. However, most of the reported results are focused on the study of reflectance and dielectric function, and to our knowledge, no study about polarization dependence has been reported.

Is Bi a semimetal that can be used for some applications based in its polarimetric response? Trying to answer this question, in this work we report on a polarization analysis of Bi thin film as a function of thickness. We have measured the complex refractive index and the Mueller matrix associated with six pure Bi thin film samples with different film thicknesses under a reflection configuration. Results show the strong sensitivity to thickness variation and to the angle of incidence, as indicated by the diattenuation and the polarizance parameter values obtained. All samples have been studied at 66.5° and 70°

1559-128X/12/368549-08$15.00/0

incidence. The pseudo-Brewster angle was found to be at 66.5° (±0.25°) incidence. One thick Bi sample was used to test the high sensitivity of the diattenuation and polarizance parameters to the angle of incidence, where it has been illuminated to 1°, 45°, 66.5°, and 70°, respectively. As a way to test the isotropy of the samples, we have rotated one sample around the normal (1.0° incidence) and have determined the anisotropic depolarization degree. To our knowledge, nobody has reported an analysis based in the Mueller–Stokes matrix formalism for Bi thin samples deposited by the laser ablation technique.

2. Mathematical Model

The linear response of a given optical system to the light intensity can be represented by the Mueller–Stokes formalism [17],

$$S^o = MS^i \Rightarrow \begin{pmatrix} s_0^o \\ s_1^o \\ s_2^o \\ s_3^o \end{pmatrix} = \begin{bmatrix} m_{00} & m_{01} & m_{02} & m_{03} \\ m_{10} & m_{11} & m_{12} & m_{13} \\ m_{20} & m_{21} & m_{22} & m_{23} \\ m_{30} & m_{31} & m_{32} & m_{33} \end{bmatrix} \begin{pmatrix} s_0^i \\ s_1^i \\ s_2^i \\ s_3^i \end{pmatrix} = \begin{pmatrix} m_{00}s_0^i + m_{01}s_1^i + m_{02}s_2^i + m_{03}s_3^i \\ m_{10}s_0^i + m_{11}s_1^i + m_{12}s_2^i + m_{13}s_3^i \\ m_{20}s_0^i + m_{21}s_1^i + m_{22}s_2^i + m_{23}s_3^i \\ m_{30}s_0^i + m_{31}s_1^i + m_{32}s_2^i + m_{33}s_3^i \end{pmatrix}, \quad (1)$$

where M stands for the Mueller matrix of the optical system represented as a square 4×4 matrix of real elements. The Mueller matrix contains information about the polarizance, diattenuation, birrefringence, depolarization, and dichroic character of the medium, among many other optical properties. In this sense, the Mueller matrix contains some kind of DNA optical character of the medium, limited only by the angles of incidence and detection employed but valid for any incident polarization state (unpolarized, partially polarized, or totally polarized). S stands for the Stokes parameter and represents any polarization state of light. It is defined in terms of the orthogonal components of the electric field vector (E_p, E_s) and their phase difference and can be written in terms of the azimuthal $(0 \le \psi \le \pi)$ and the ellipticity $(-\pi/4 \le \chi \le \pi/4)$ angles of the polarization ellipse of the wave, respectively [17].

A very important property associated with an optical system is its capacity to depolarize the incident light. This characteristic is determined usually through the depolarization scalar metrics.

In this work we will use the depolarization index DI, and some auxiliary parameters like the diattenuation D, the linear diattenuation D_L, the circular diattenuation D_C, the polarizance P, the linear polarizance P_L, and the circular polarizance P_C [17–20]. We will also use the $Q(M)$ metric [21–23] and the well-known degree of polarization, DoP. The anisotropic degree of depolarization, Add, is a relationship that gives insight into the isotropy or anisotropy depolarization capacity of the medium. It has been defined by [24]

$$0 \le \mathrm{Add} = \frac{(\mathrm{DoP})^o_{\mathrm{Max}} - (\mathrm{DoP})^o_{\mathrm{min}}}{(\mathrm{DoP})^o_{\mathrm{Max}} + (\mathrm{DoP})^o_{\mathrm{min}}} \le 1, \quad (2)$$

where $(\mathrm{DoP})^o$ indicates the output degree of polarization from the sample.

By following an analogy with the previous polarization metric, the anisotropic gain degree, Agd, can be defined for passive systems by

$$0 \le \mathrm{Agd} = \frac{(g)^o_{\mathrm{Max}} - (g)^o_{\mathrm{min}}}{(g)^o_{\mathrm{Max}} + (g)^o_{\mathrm{min}}} \le 1. \quad (3)$$

This quantity can be used as a measure of the output gain [25] dependence on the incident polarization state, and its lower physical limit could be associated with a passive, isotropic response of the medium to any incident polarization state.

There are many methods reported for the determination of the Mueller matrix elements based on the measurement of the Stokes vectors for the incident and scattered light from the sample [17,26,27]. For a general optical system, all of the reported methods are based on the generation and detection of polarization states, by applying Eq. (1), in order to build a minimum of 16 linear equations with 16 unknown. The Mueller matrix is obtained once the simultaneous equations are solved for each m_{ij} $(i, j = 0, 1, 2, 3)$. We suggest that interested readers review some of the papers cited in [17].

The effective medium approximation is a formulation valid for one single interface system (one boundary that separates two media). This approximation can be applied to thin film systems if the thickness of the propagating medium is greater than or equal to five times the skin depth associated with the incident wavelength. Considering a transparent/absorbing interface, the complex refraction index (n, k) can be expressed in terms of the ellipsometric parameter $\rho(\psi, \Delta)$ [28]:

$$n = \mathrm{Re}\left\{\tan\theta_i\left[1 - \frac{4\rho}{(1+\rho)^2}\sin^2\theta_i\right]^{1/2}\right\},$$
$$k = \mathrm{Im}\left\{\tan\theta_i\left[1 - \frac{4\rho}{(1+\rho)^2}\sin^2\theta_i\right]^{1/2}\right\}, \quad (4a)$$

where

$$\rho(\lambda) = \tan\psi \exp(i\Delta), \quad \tan\psi = \left|\frac{r_p}{r_s}\right|, \quad \Delta = \delta_{r_p} - \delta_{r_s}, \quad (4b)$$

and r_p and r_s are the Fresnel reflection coefficients associated with the parallel and perpendicular components, respectively [28].

The skin depth is a measure of the capacity of penetration of the incident light into a sample, and it is given by the relationship [28]

$$\text{Skin depth} = \frac{\lambda}{4\pi\kappa}[\text{nm}], \qquad N = n - ik, \qquad (5)$$

where k is the extinction coefficient (imaginary part of the complex refraction index, N) and λ is the incident wavelength.

3. Thin Film Preparation

Laser ablation was performed using a Q-switched Nd:YAG laser with emission at the fundamental line (1064 nm) with a 5 ns pulse duration and 10 Hz repetition rate. The laser beam was focused on a rotating high purity Bi target (plasmaterials 99.99%). The energy density (fluence) delivered to the target was fixed at 3 J/cm^2. The target and the substrates were placed in a vacuum chamber evacuated to a base pressure of 1.3×10^{-4} Pa, and all the samples were deposited at this pressure. The Bi thin films were deposited on small pieces (1.5 cm × 1.5 cm) of flat pyrex glass previously cleaned in an ultrasonic bath of methanol. The distance between the substrate and target was fixed at 6 cm. All depositions were made at room temperature.

In the experimental conditions described, the mean kinetic ion energy of the Bi^+ and the plasma density took the values of 90 eV and 3.3×10^{13} cm^{-3}, respectively. These values were determined using a Langmuir planar probe and were kept constant for the deposited samples. The measurements of the Langmuir probe assure a good reproducibility of the experiments.

In order to obtain samples with different thicknesses, the deposition time was varied, taking into account the fact that in the described experimental conditions, the deposition rate was 12 nm/min. For the studies described in this paper, there were deposited six samples with the following thicknesses: 180, 160, 103, 91, 66, and 60 nm. The thickness of each sample was measured using a stylus-type profilometer (Veeco-Bruker, Dektak 6M).

Structural and compositional analysis were performed on some of the deposited samples. Figure 1 shows the x-ray diffraction pattern of the thicker sample, consisting of only two diffraction peaks. From this figure the crystalline structure of the film with a preferred orientation on the (003) direction can be observed. Using this diffractogram and the Scherer equation, a grain size of 35 nm was obtained. The grain size is a function of the Bi ion energy used for deposition of the films. For low values of the ion energy, up to 200 eV, the grain size takes values around 35 nm, and for higher values of the ion energy, the grain size increases. It is worth noting that in the present experiment we studied samples with different thicknesses but deposited in the same experimental conditions, so that the Bi ion energy was kept constant at a value close to 90 eV. In [14], the authors report a grain size of few micrometers for Bi thin film growth on Si substrates with an energy density delivered to the target fixed at 2 J/cm^2 and a separation distance of 33 mm between the source and

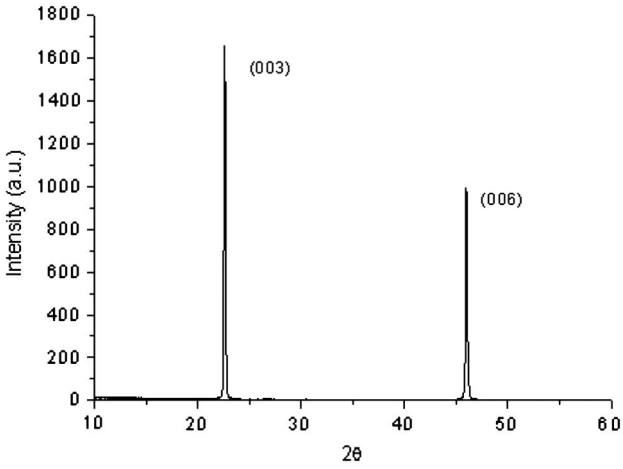

Fig. 1. X-ray diffraction pattern of a Bi thin film with 180 nm thickness and grain size of 35 nm.

substrate. We believe the difference in grain size is due to the different conditions employed with the deposition process. The compositional analysis was carried out using Rutherford backscattering spectrometry. The results obtained for the samples studied here showed the presence of Bi and no other elements, up to the accuracy of the method (of about 3 at. %); however, there is probably the presence of oxygen on the surface. From these measurements it was also possible to obtain a value of 8.9 g/cm^3 for the density of the material. Figure 2 shows the compositional analysis obtained using Rutherford backscattering spectrometry, where two oxidized Bi samples are compared with a pure Bi sample. The presence of oxygen can be observed on the two thicker thin films (422 and 555 nm, not studied here).

4. Results

To evaluate the skin depth of the studied samples [see Eq. (5)], the complex refraction index has been

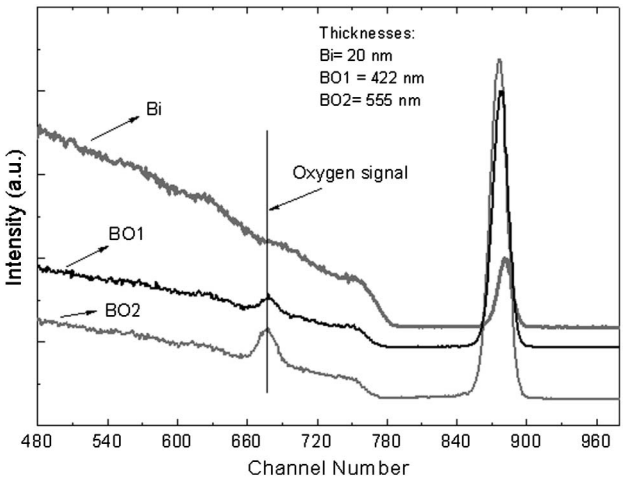

Fig. 2. Rutherford backscattering spectra of pure Bi thin film (20 nm thickness), compared with the spectra obtained from two Bi oxide thin films (BO1 and BO2) with different thicknesses. The absence of oxygen signal in the case of the pure Bi thin film is observed.

measured for the six samples and for the thicker sample after 6 months (which shows direct visual evidence of a slight oxidation) (see Fig. 3). The ellipsometric parameters (ψ, Δ) have been determined with a spectroscopic ellipsometer (Angstrom Advanced Inc, model PHE-102), at 70° incidence. Figure 3 shows the real (n) and the imaginary (k) parts of the complex refraction index, measured from 250 to 1100 nm, once Eq. (4) has been applied to the ellipsometric parameters.

Observe from Fig. 3 a noisy response at lower incident wavelengths (UV region), which decreases with thickness increase (this could be due to surface morphological changes). Note that all the films with thicknesses lower than or equal to 103 nm show very similar behavior, which differs notably from the samples with greater thickness. Samples with a thickness of 160 and 180 nm show similar behavior in k for the entire wavelength range studied here; however, the thinner of them increases its value with increasing wavelength in n. The thicker sample shows a slight variation in the real part of the refractive index with oxidation; however, it presents a notable change in the imaginary part (maintains the same shape, but with a lower value). Our results are similar to those reported in [14–16] and the references therein for Bi thin films equal to or lower than 103 nm, in the range 300–800 nm. We do not understand why the two thicker films have lower values for the complex refractive index with respect to those reported for the bulk crystalline Bi [29], considering our samples were grown without oxygen.

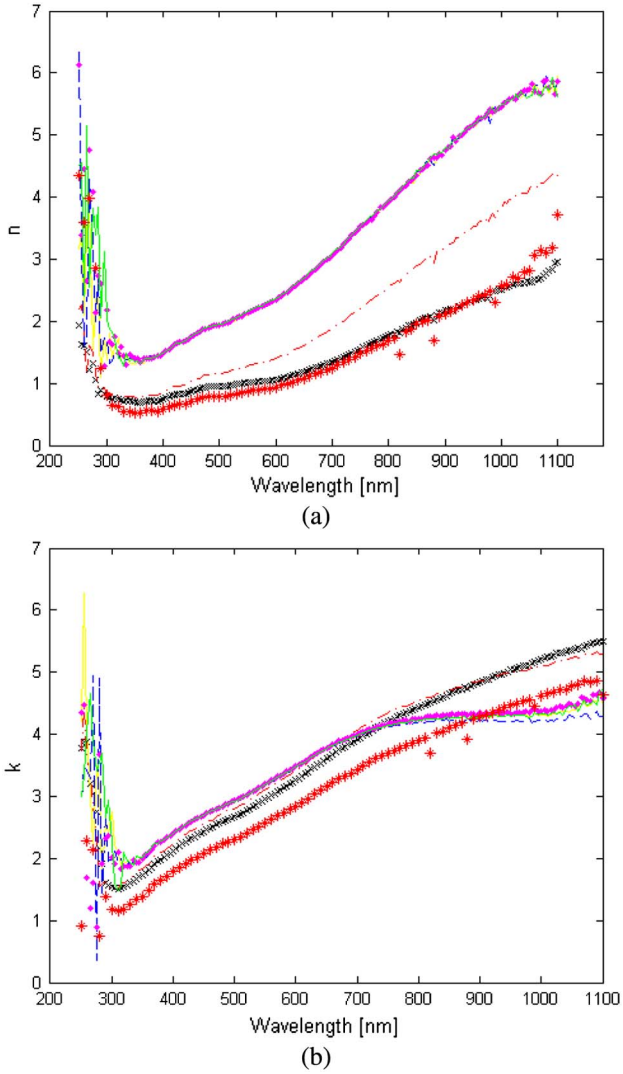

Fig. 3. (Color online) (a) Real (n) and (b) imaginary (k) parts of the refractive index of Bi, as a function of wavelength, obtained in PLD films of different thicknesses. x's represent 180 nm (black); dash-dotted curve, 160 nm (red); solid curve, 103 nm (yellow); dashed curve, 91 nm (blue); dotted curve, 66 nm (magenta); solid curve, 60 nm (green); and asterisks, 180 nm (red), measured 6 months later (oxide overlayer not determined). Results obtained are similar to those reported in [14–16] and references therein for samples with thicknesses lower than or equal to 103 nm. Data has been taken at 70° incidence.

The illumination wavelength used in this work (632.8 nm) for the determination of the Mueller matrix gives a skin depth of 13.94 nm [Eq. (5)]. This suggests that the polarimetric parameters measured provide information about the surface behavior of thin film, because the illumination never reaches the second interface of the system (Bi thin film–glass substrate). In other words, the system behaves as a simple system: air–Bi thin film.

If the minimum intensity reflected by a plane surface is zero when a linear p-polarization state (E_p) illuminates the surface, then the incidence angle is called the Brewster angle. An incident unpolarized state can be s-linearly polarized under reflection by a flat surface if the incidence occurs at the Brewster (or polarization) angle. We have found the minimum nonzero intensity value reflected by each sample when a p-linearly polarized state is employed. This is the pseudo-Brewster angle and occurs at 66.5° (see Fig. 4).

Observe that the bottom plane in Fig. 4 represents all the possible incident polarization states on the Bi sample, and the surface represents the output degree of polarization response associated with each of them. If a totally polarized output state is required, then an s-incident polarization state must be employed (zero degrees for both, the azimuth and the ellipticity angles), among many other possibilities. This means that the information provided by surfaces, such as the degree of polarization, can be used to handle the output response of the system under study as a function of the incident polarization state. This is the principle for designing possible photonic Bi-based devices for several applications.

The Mueller matrix has been determined for six different samples of pure Bi thin films deposited by the laser ablation technique. A commercially available polarimeter (Thorlabs, PAN5720VIS) has been employed to analyze the reflected light from the samples for each of the six different polarization states used for the incidence [linear parallel, p, perpendicular, s, +45 and −45, and right-hand (r) and left-hand (l) circular polarization states]. A fixed

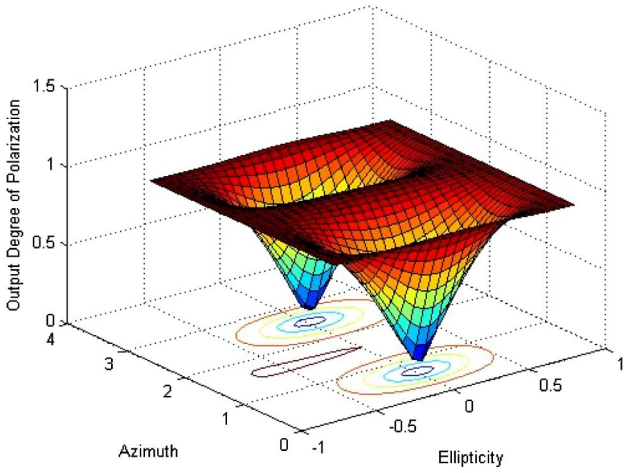

Fig. 4. (Color online) Polarimetric optical response of Bi thin film sample (160 nm thickness) versus incident polarization state. An illumination of 632.8 nm of continuous wavelength was employed at 66.5° incidence (the pseudo-Brewster angle).

Glan–Thompson polarizer and an azimuth-angle-rotatable liquid-crystal variable phase retarder (Thorlabs, LCR-1-VIS) have been used as the polarization state generator. We have chosen 66.5° and 70° as the incidence angles, the first because it is associated to the pseudo-Brewster angle, which is interesting *per se*, and the second because it is the angle at which the spectro-ellipsometric characterization is usually reported for Bi thin films [1] and could be used as a matter of reference.

The Mueller matrix associated with each sample is shown in Appendix A. Table 1 shows the results obtained when the scalar metrics are applied to the Mueller matrices (Appendix A).

The polarimeter employed has a resolution of 0.0001 for the Stokes vectors, the same as for the values calculated in Table 1. From Table 1, it can be observed that at the pseudo-Brewster angle (66.5°), all the samples show a tendency to reach a constant and similar value for the diattenuation, D, mainly the linear diattenuation, D_L. An analogous behavior is observed for the polarizance parameter, P, and for the linear polarizance, P_L. This value seems to be located inside the interval (0.26–0.28), independent of the sample thickness. More detailed information could be obtained if we were able to have access to additional samples with intermediate and additional thickness values.

However, it can be observed that for an incident illumination at 70°, both of these parameters, D (D_L) and P (P_L), take on increased values (also very similar to each other) as the thickness decreases. This can be interpreted as the existence of a strongly dependent response of Bi thickness on the incident polarization. We believe the polarimetric changes are due to the variable surface quality with film thickness; this can be supposed indirectly from the increase of noise at higher energies (lower wavelengths) of incidence, according to Fig. 3. In this sense, the increase in the anisotropic gain degree value, Agd [Eq. (3)], is also consistent with the interpretation given to the diattenuation and means that the absorption increases with the roughness decrease, with a strong dependence on the incident polarization states.

Notice that the circular diattenuation, D_C, and the circular polarizance, P_C, do not follow a clear behavior with roughness variation. At the pseudo-Brewster angle, the remaining metrics provide inconsistent results, which could be associated with a random response due to the small surface roughness present at the surface Bi thin films (the beam forms an elliptical spot on the surface, which means several grains are illuminated, resulting in a random orientation of radiating dipoles around the specular direction).

On the other hand, the application of the depolarization index, DI, shows that all samples depolarize light very slightly. The $Q(M)$ metric values are associated with diattenuating, very slightly depolarizing systems, valid for all the samples. The values are reported as obtained experimentally, without noise or error correction. This is the reason for the appearance of a small noise value for the depolarization index, DI, which takes on values up the physical limit. This behavior does not change the tendency associated with the diattenuation and the polarizance parameters.

Table 1. Polarimetric Data as a Function of Bi Thin Film Thickness at Incidence Angles of 66.5° (pseudo-Brewster Angle) and 70°, Respectively[a]

Incidence Angle (deg)	D	D_L	D_C	P	P_L	P_C	DI	Add	Agd	$Q(M)$
66.5/70 A: Bi6-1/180 nm	0.2702/	0.2676/	0.0373/	0.2604/	0.2604/	0.0063/	1.0052/	0.0340/	0.1633/	2.7571/
	0.2946	0.2939	0.0207	0.2889	0.2888	0.0065	0.9951	0.0304	0.1796	2.6535
66.5/70 B: Bi6-4/160 nm	0.2689/	0.2687/	0.0102/	0.2694/	0.2685/	0.0220/	0.8245/	0.1729/	0.1641/	1.8344/
	0.2956	0.2956	0.0000	0.2957	0.2950	0.0196	1.0015	0.0165	0.1805	2.6867
66.5/70 C: NBC9/103nm	0.2785/	0.2785/	0.0000/	0.2781/	0.2776/	0.0171/	1.0018/	0.0153/	0.1700/	2.7222/
	0.3080	0.3080	0.0035	0.3080	0.3076	0.0163	1.0013	0.0143	0.1880	2.6606
66.5/70 D: NBC8/91 nm	0.2774/	0.2773/	0.0035/	0.2774/	0.2768/	0.0181/	0.9997/	0.0130/	0.1693/	2.7127/
	0.3099	0.3099	0.0012	0.3100	0.3093	0.0201	1.0002	0.0127	0.1892	2.6504
66.5/70 E: NBC10/66 nm	0.2632/	0.2632/	0.0036/	0.2638/	0.2630/	0.0205/	1.0132/	0.0116/	0.1608/	2.8152/
	0.3141	0.3119	0.0374	0.3120	0.3114	0.0201	0.9852	0.0133	0.1904	2.5607
66.5/70 F: NBC11/60 nm	0.2753/	0.2753/	0.0023/	0.2752/	0.2746/	0.0192/	0.9291/	0.3486/	0.1680/	2.3366/
	0.3134	0.3134	0.0070	0.3134	0.3131	0.0132	0.9178	0.1266	0.1912	2.2115

[a]An illumination of 632.8 nm of continuous wavelength was employed.

Table 2. Polarimetric Data of Sample A (Bi6-1, 180 nm) as a Function of the Surface Polarization Isotropy[a]

Position (deg)	0, 360	45	90	135	180	225	270	315
D	0.0060	0.0310	0.0220	0.0105	0.0336	0.0105	0.0118	0.0136
P	0.0119	0.0161	0.0212	0.0292	0.0234	0.0181	0.0251	0.0294
DI	0.9890	0.9955	0.9963	0.9925	0.9911	0.9937	0.9941	0.9925
$Q(M)$	2.9344	2.9693	2.9761	2.9546	2.9425	2.9620	2.9642	2.9546
Add	0.0161	0.0273	0.0319	0.0412	0.0389	0.0373	0.0384	0.0413

[a]An illumination of 632.8 nm of continuous wavelength was employed at a near-normal incidence.

Table 3. Polarimetric Data of Sample A (Bi6-1, 180 nm) as a Function of the Incidence Angle[a]

Incidence Angle (deg)	D	P	DI	$Q(M)$	Add
1	0.0336	0.0234	0.9911	2.9425	0.0389
45	0.1199	0.1213	1.0019	2.9543	0.0370
66.5	0.2702	0.2604	1.0052	2.7571	0.0395
70	0.2946	0.2889	0.9951	2.6535	0.0401

[a]An illumination of 632.8 nm of continuous wavelength was employed.

We have also analyzed the surface isotropic polarization response of samples from the Mueller matrix. In Table 2 we present some polarimetric characteristic values associate with sample A (Bi6-1, 180 nm) at an incidence angle of 1.0° when the sample surface is rotated from 0° to 360° by steps of 45° around the normal to the surface. The initial orientation is arbitrarily chosen along one side of the square substrate, and the corresponding Mueller matrices are not reported here.

Observe that there is an almost symmetric direction along the angles 135° and 315°, where the polarizance, the depolarization index, the $Q(M)$ metric, and the anisotropic depolarization degree take the same values, even when there is a small difference between the values of the diattenuation parameters along the opposite directions. The origin of the reference system has been chosen as the spot on the illuminated surface. Observe also, there is a strong dependence of the diattenuation on polarization along the directions 45° and 180°; this behavior could be associated with the nonsymmetric orientation and shape of the Bi grains with respect to the normal to the surface. The sample depolarizes light very slightly, and the physical limits are respected; this means that the Mueller matrix has been well-determined at incidences close to the normal. At larger angles of incidence, the beam reflected increases its transversal section, originating problems at the analyzing optical head, which accepts beams within a 3 mm diameter. This also depends on the surface morphology, because a greater grain size originates a greater scattering of light. Table 2 shows the existence of a surface morphology anisotropic response to polarization of light.

Finally, the previous sample, A, is used to test the high sensitivity of the diattenuation and the polarizance parameters to the angle of incidence. Sample A has been illuminated at 1°, 45°, 66.5°, and 70° incidence, respectively, and the Mueller matrix has also been obtained at each angle. Table 3 shows the results obtained when some scalar metrics are applied to the Mueller matrices obtained under the illumination conditions cited before.

Notice that the diattenuation and the polarizance parameters increase with the increase of the incidence angle, while the sample depolarizes the incident light very slightly at an almost stationary value, according to Add. In this case, the surface position of the sample at 180°, reported in Table 2, was oriented parallel to the plane of incidence.

5. Conclusions

We have measured the complex refractive index and the Mueller matrix associated with six pure Bi thin film samples with different thicknesses. Results of the complex refractive index are similar to those reported in [14–16] for thin films with thicknesses equal to or lower to 103 nm, which proves indirectly that our samples are not oxidized. For comparison, we have measured the thicker film 6 months after, and results on the imaginary part of the complex refractive index show the presence of oxidation (overlayer thickness has not been determined). Results also show that the diattenuation and the polarizance parameters are very sensitive to thickness variation and also to the incident angle. Samples have been studied at 66.5° and 70° incidence, respectively. The pseudo-Brewster angle has been found to be at 66.5° incidence. The surface isotropic polarization response of a sample has been presented. The skin depth value associated with the illumination employed, 632.8 nm, permits us to suggest that the polarization response obtained is a consequence of surface morphology changes with the thin film thickness variation. We believe the laser ablation deposition technique could be used to get pure Bi thin film samples, able to be used for different photonic applications at room conditions. By knowing the polarimetric response of Bi thin films, through the Mueller matrix, the use of appropriate incident polarization states could be used to design photonic devices for several applications.

Appendix A

Included is the experimental normalized Mueller matrix associated with the Bi thin film samples deposited by the ablation laser technique. The samples are illuminated to incidence angles at the pseudo-Brewster angle (66.5°) and to 70°, respectively. Samples A, B, C, D, E, and F are associated with 180, 160, 103, 91, 66, and 60 nm thickness, respectively.

$$M_{A,66.5} = \begin{bmatrix} 1.0000 & -0.2672 & -0.0117 & 0.0373 \\ 0.0953 & -0.3737 & 0.5274 & -0.7695 \\ -0.2423 & 0.9237 & 0.1929 & -0.3697 \\ 0.0063 & -0.0063 & -0.7673 & -0.5146 \end{bmatrix},$$

$$M_{B,66.5} = \begin{bmatrix} 1.0000 & -0.2684 & 0.0114 & -0.0102 \\ -0.2684 & 0.9969 & -0.0020 & 0.0623 \\ 0.0046 & -0.0698 & 0.0062 & 0.8102 \\ 0.0220 & -0.0253 & 0.0096 & -0.4844 \end{bmatrix},$$

$$M_{C,66.5} = \begin{bmatrix} 1.0000 & -0.2780 & 0.0173 & 0.0000 \\ -0.2775 & 0.9980 & -0.0666 & 0.0435 \\ 0.0085 & -0.0516 & -0.5934 & 0.7700 \\ 0.0171 & -0.0278 & -0.7531 & -0.5815 \end{bmatrix},$$

$$M_{D,66.5} = \begin{bmatrix} 1.0000 & -0.2769 & 0.0150 & 0.0035 \\ -0.2768 & 0.9976 & -0.0684 & 0.0432 \\ 0.0061 & -0.0566 & -0.6974 & 0.7638 \\ 0.0201 & -0.0288 & -0.7484 & -0.5816 \end{bmatrix},$$

$$M_{E,66.5} = \begin{bmatrix} 1.0000 & -0.2631 & 0.0070 & -0.0036 \\ -0.2629 & 0.9976 & -0.0647 & 0.0480 \\ 0.0059 & -0.0577 & -0.6168 & 0.7826 \\ 0.0205 & -0.0280 & -0.7534 & -0.6118 \end{bmatrix},$$

$$M_{F,66.5} = \begin{bmatrix} 1.0000 & -0.2748 & 0.0161 & -0.0023 \\ -0.2745 & 0.9988 & -0.0666 & 0.0450 \\ 0.0069 & -0.0564 & -0.6122 & 0.7413 \\ 0.0192 & -0.0274 & 0.3911 & -0.5939 \end{bmatrix},$$

$$M_{A,70} = \begin{bmatrix} 1.0000 & -0.2939 & -0.0049 & 0.0207 \\ 0.1017 & -0.3771 & 0.3661 & -0.8263 \\ -0.2704 & 0.9200 & 0.1211 & -0.3727 \\ 0.0065 & -0.0065 & -0.8623 & -0.3127 \end{bmatrix},$$

$$M_{B,70} = \begin{bmatrix} 1.0000 & -0.2949 & 0.0208 & 0.0000 \\ -0.2950 & 0.9973 & -0.0604 & 0.0613 \\ 0.0033 & -0.0638 & -0.3420 & 0.8971 \\ 0.0196 & -0.0294 & -0.8929 & -0.3288 \end{bmatrix},$$

$$M_{C,70} = \begin{bmatrix} 1.0000 & -0.3075 & 0.0173 & -0.0035 \\ -0.3075 & 0.9987 & -0.0611 & 0.0465 \\ 0.0057 & -0.0474 & -0.4499 & 0.8491 \\ 0.0163 & -0.0310 & -0.8361 & -0.4349 \end{bmatrix},$$

$$M_{D,70} = \begin{bmatrix} 1.0000 & -0.3096 & 0.0138 & -0.0012 \\ -0.3093 & 0.9977 & -0.0614 & 0.0483 \\ 0.0038 & -0.0518 & -0.4541 & 0.8455 \\ 0.0201 & -0.0324 & -0.8316 & -0.4371 \end{bmatrix},$$

$$M_{E,70} = \begin{bmatrix} 1.0000 & -0.3116 & 0.0127 & 0.0374 \\ -0.3114 & 0.9977 & -0.0597 & 0.0326 \\ 0.0041 & -0.0518 & -0.4634 & 0.7951 \\ 0.0201 & -0.0318 & -0.8273 & -0.4254 \end{bmatrix},$$

$$M_{F,70} = \begin{bmatrix} 1.0000 & -0.3127 & 0.0207 & 0.0070 \\ -0.3130 & 0.9995 & -0.0641 & 0.0410 \\ 0.0055 & -0.0496 & -0.4640 & 0.8367 \\ 0.0132 & -0.0328 & -0.4507 & -0.4513 \end{bmatrix}.$$

The research leading to these results has received funding from the CONACYT under grant agreements 100361, 263878, and 125141, respectively, and from the European Community Seven Framework Programme (FP7-NMP-2010-EU-MEXICO).

References

1. O. Hunderi, "Optical properties of crystalline and amorphous bismuth films," J. Phys. F **5**, 2214–2225 (1975).
2. S. Golin, "Band structure of bismuth: pseudopotential approach," Phys. Rev. **166**, 643–651 (1968).
3. M. Cardona and D. L. Greenaway, "Optical properties and band structure of group IV–VI and group V materials," Phys. Rev. **133**, A1685–A1697 (1964).
4. A. P. Lenham, D. M. Treherne, and R. J. Metcalfe, "Optical properties of antimony and bismuth crystals," J. Opt. Soc. Am. **55**, 1072–1074 (1965).
5. J. Toots and L. Marton, "Optical properties of antimony and bismuth in the far ultraviolet," J. Opt. Soc. Am. **59**, 1305–1308 (1969).
6. S. Dogel, D. Nattland, and W. Freyland, "Complete wetting transitions at the liquid-vapor interface of gallium-bismuth alloys: single wavelength and spectroscopic ellipsometry studies," Phys. Rev. B **72**, 085403 (2005).
7. O. Rabin, J. M. Perez, J. Grimm, G. Wojtkiewicz, and R. Weissleder, "An x-ray computed tomography imaging agent based on long-circulating bismuth sulphide nanoparticles," Nat. Mater. **5**, 118–122 (2006).
8. M. V. Yezhelyev, X. Gao, Y. Xing, A. Al-Hajj, S. Nie, and R. M. O'Regan, "Emerging use of nanoparticles in diagnosis and treatment of breast cancer," Lancet Oncol. **7**, 657–667 (2006).
9. R. Venkatasubramanian, E. Siivola, T. Colpitts, and B. O'Quinn, "Thin-film thermoelectric devices with high room-temperature figures of merit," Nature **413**, 597–602 (2001).
10. A. Ghosh, "Memory switching in bismuth-vanadate glasses," J. Appl. Phys. **64**, 2652–2655 (1988).
11. I. Svancara, C. Prior, S. B. Hocevar, and J. Wang, "A decade with bismuth-based electrodes in electroanalysis," Electroanalysis **22**, 1405–1420 (2010).
12. G. Fuchs, C. Montandon, M. Treilleux, J. Dumas, B. Cabaud, P. Mélinon, and A. Hoareau, "Low-energy Bi cluster beam deposition," J. Phys. D **26**, 1114–1119 (1993).
13. R. Atkinson and E. Curran, "Ellipsometric examination of the oxidation of vacuum-deposited bismuth films," Thin Solid Film **128**, 333–339 (1985).
14. J. C. G. de Sande, T. Missana, and C. N. Afonso, "Optical properties of pulsed laser deposited bismuth films," J. Appl. Phys. **80**, 7023–7027 (1996).
15. R. Serna, J. C. G. de Sande, J. M. Ballesteros, and C. N. Afonso, "Spectroscopic ellipsometry of composite thin films with embedded Bi nanocrystals," J. Appl. Phys. **84**, 4509–4516 (1998).
16. D. Liu, K. Wu, M. Shih, and M. Chern, "Giant nonlinear optical properties of bismuth thin films grown by pulsed laser deposition," Opt. Lett. **27**, 1549–1551 (2002).

17. D. Goldstein, *Polarized Light*, 3rd ed. (CRC, 2011).
18. J. J. Gil and E. Bernabeu, "A depolarization criterion in Mueller matrices," Opt. Acta **32**, 259–261(1985).
19. J. J. Gil and E. Bernabeu, "Depolarization and polarization indexes of an optical system," Opt. Acta **33**, 185–189 (1986).
20. S. Y. Lu and R. A. Chipman, "Mueller matrices and the degree of polarization," Opt. Commun. **146**, 11–14 (1998).
21. R. Espinosa-Luna and E. Bernabeu, "On the $Q(M)$ depolarization metric," Opt. Commun. **277**, 256–258 (2007).
22. S. Savenkov, A. Priezzhev, Ye. Oberemok, P. Silfsten, T. Ervasti, J. Ketolainen, and K. E. Peiponen, "Characterization of porous media by means of the depolarization metrics," J. Quant. Spectrosc. Radiat. Transfer **113**, 2503–2511 (2012).
23. R. Espinosa-Luna, G. Atondo-Rubio, and O. J. Velarde-Escobar, "Métrica de despolarización escalar $Q(M)$ como criterio para identificar sistemas retardadores o desfasadores puros," Rev. Mex. Fis. **56**, 406–410 (2010).
24. P. Eliés, B. Le Jeune, F. Le Roy-Brehonnet, J. Cariou, and J. Lotrian, "Optical media and target characterization by Mueller matrix decomposition," J. Phys. D **29**, 34–38 (1996).
25. C. Brosseau, *Fundamentals of Polarized Light: A Statistical Optics Approach* (Wiley, 1998).
26. R. Espinosa-Luna, "Scattering by rough surfaces in a conical configuration: experimental Mueller matrix," Opt. Lett. **27**, 1510–1512 (2002).
27. K. M. Salas-Alcántara, R. Espinosa-Luna, and I. Torres-Gómez, "Polarimetric Mueller–Stokes analysis of photonic crystal fibers with mechanically-induced long-period gratings," Opt. Eng. **51**, 085005 (2012).
28. H. Fujiwara, *Spectroscopic Ellipsometry: Principles and Applications* (Wiley, 2007).
29. P. Y. Wang and A. L. Jain, "Modulated piezoreflectance in bismuth," Phys. Rev. B **2**, 2978–2983 (1970).